Performance Analysis of Reconfigurable Antenna Arrays

Rajitha Senanayake, *Member, IEEE*, Peter J. Smith, *Fellow, IEEE*, Philippa A. Martin, *Senior Member, IEEE*, and Jamie S. Evans, *Member, IEEE*

***Abstract*— Reconfigurable antenna arrays provide a means for efficient use of the spatial domain in wireless communication systems. Despite its potential, the topic is only briefly explored in the literature. In this paper, we present a comprehensive theoretical analysis of the performance of reconfigurable systems. We consider a receiver equipped with multiple reconfigurable antennas that pick the best state based on the channel between the transmitter and the receiver. For such a system, we derive a new expression for the moment generating function (MGF) of the received signal-to-noise ratio by employing maximal ratio combining. Based on the MGF, we analyze three important performance measures, specifically, achievable rate, error probability, and outage probability. Furthermore, we conduct an asymptotic analysis incorporating the correlation between reconfigurable states and show that a reconfigurable system can achieve a diversity order of the number of antennas times the number of reconfigurable states. Finally, we discuss the applicability of reconfigurable antennas in novel wireless networks with large antenna arrays and distributed antenna systems, highlighting the performance gains and requirement for fewer RF chains.**

***Index Terms*— Reconfigurable antenna arrays, maximal ratio combining, antenna selection, Rayleigh fading.**

I. Introduction

EMPLOYING multiple antennas at the receiver has been shown to improve network performance since the early days of wireless communications. With the time and frequency domain resources largely utilized to accommodate the increasing user demand, the efficient use of the *spatial domain* is essential for wireless communications. Although the addition of multiple antennas at the base station is desirable, its deployment poses new practical challenges in-terms of fabrication costs, space requirements and power consumption. While the physical antennas and the additional digital signal processing components are cheap, the radio frequency (RF) chain that consists of the power amplifier, mixer, digital to analogue converter and filter is expensive [1]. Moreover, the signal processing complexity and power consumption of the base station significantly increases with increasing number of RF chains [2]. Thus, a major challenge in future multi-antenna wireless networks is the design of communication schemes with a limited number of RF chains.

Fueled by these considerations, the principle of antenna selection at the transmitter and receiver has garnered much research attention in past years [3]–[9]. This strategy consists of selecting a subset of the available antennas to optimally assign the limited number of RF chains. Regardless of its conceptual simplicity, antenna selection suffers from a number of drawbacks. Firstly, an antenna capable of element selection requires well-matched and response-stable microwave switches that are expensive [10]. Secondly, the distance between the elements must be in the order of a half wave-length to avoid strong coupling, which is problematic when implementing large antenna arrays [11].

Reconfigurable antennas offer a different approach to efficiently utilize the spatial domain with a fixed hardware complexity in terms of the physical antennas and RF chains. Reconfiguring an antenna is achieved through deliberately adapting the frequency, polarization or radiation pattern characteristics [12]–[14]. This allows the propagation channels to be altered dynamically, to experience different channel conditions which we call reconfigurable states. Each physical antenna selects the best state from the group of reconfigurable states based on the channel parameters [10]. Thus, a key advantage of the reconfigurable system is the reduced number of physical antennas required when compared to antenna selection. Moreover, the RF chains can be fixed to the physical antennas since no element selection is required.

The use of reconfigurable antennas in wireless networks has recently attracted a lot of attention due to the additional degrees of freedom they offer based on these reconfigurable states. One can imagine each state as a different *virtual* antenna that may experience different radiation pattern characteristics. Various implementation mechanisms and design approaches have been developed to achieve reconfigurability [14]–[20]. Electrically reconfigurable antennas that rely on RF micro electromechanical systems (MEMS) [15], [16], PIN diodes [17] or varactors [18] redistribute surface currents to alter the radiating structure topology. Optically reconfigurable antennas rely on photoconductive switching elements [19] while physically reconfigurable antennas alter the radiating structure [20]. Smart materials such as ferrites and liquid crystals can also be used to create different states through a change

Manuscript received July 6, 2016; revised November 16, 2016; accepted March 3, 2017. Date of publication March 15, 2017; date of current version June 14, 2017. The associate editor coordinating the review of this paper and approving it for publication was M. Uysal.

R. Senanayake and J. S. Evans are with the Department of Electrical and Electronic Engineering, University of Melbourne, Melbourne, VIC 3010, Australia (e-mail: rajitha.senanayake@unimelb.edu.au; jse@unimelb.edu.au).

P. J. Smith is with the School of Mathematics and Statistics, Victoria University of Wellington, Wellington 6012, New Zealand (e-mail: peter.smith@vuw.ac.nz).

P. A. Martin is with the Department of Electrical and Computer Engineering, University of Canterbury, Christchurch 8041, New Zealand (e-mail: philippa.martin@canterbury.ac.nz).

Color versions of one or more of the figures in this paper are available online at http://ieeexplore.ieee.org.

Digital Object Identifier 10.1109/TCOMM.2017.2682081

in the substrate characteristics [14]. Reconfigurable antennas can also be classified according to the antenna parameter that is dynamically adjusted. A frequency/polarization reconfigurable antenna is able to change the frequency/polarization of operation. A radiation pattern reconfigurable antenna is able to tune the radiation pattern. They are extensively used for beam steering [21], [22]. A hybrid reconfiguration can also be achieved by simultaneously tuning several antenna parameters. In this paper, we take a general approach and model different channels created by the reconfigurable states rather than focusing on a specific enabling technology.

Despite its potential, fairly little analytical work on reconfigurable antenna arrays is available in the literature. Many studies rely on simulations. In [10], a reconfigurable antenna array system is proposed that employs tunable parasitic elements that are adaptively modified to maximize the channel capacity. Numerical and experimental results illustrate the significant improvement in the system capacity with a minimum impact on the hardware complexity. In [23], another electronically steerable reconfigurable antenna array system is studied to achieve increased spectral efficiency characteristics. Some analytical progress has been made in [24] and [25]. In [24], the amount of signal-to-noise ratio (SNR) scaling offered by the reconfigurable antennas is studied. It was shown that the reconfigurable model can provide at least 76% of the improvements offered by antenna selection. However, the gain in antenna selection may not be warranted as it demands more physical antennas and adaptable antenna feeds.

Note that the reconfigurable system can be viewed as a restricted version of antenna selection While the receiver with antenna selection has full flexibility to select the set of antennas experiencing the best channels out of *all* the available antennas, with reconfigurable antennas the selection is limited to each antenna choosing a reconfigurable state from a set. This forms a mathematical problem which, unlike antenna selection, relies on maximal order statistics from several sets of states.

In this paper, we carry out a comprehensive analysis on the performance of a reconfigurable antenna array system where each antenna at the receiver side has multiple reconfigurable states. In each coherence time, the receive antennas select the state that experiences the best channel. The signals received through these channels are then combined using the standard maximum ratio combining (MRC). As such, the system can be viewed in two steps, first selection combining (SC) applied to a subset of channels followed by MRC - two well-known combining techniques when considered separately. However, when combined together it creates a new channel structure which is far more complex than conventional MRC or SC. The MRC output has a new statistical distribution and a novel, more advanced analysis is required for system performance evaluation. The contributions of our paper are detailed as follows:

- We derive a new closed-form expression for the moment generating function (MGF) of the instantaneous received SNR when the channels are subject to Rayleigh fading. Our MGF expression permits intuitive characterizations of three important performance measures namely, the achievable rate, symbol error probability (SEP) and outage probability of the transmitter.
- We conduct an asymptotic analysis based on the correlated case where the channels experienced by the reconfigurable states within each antenna are not independent. Based on the high SNR approximations on the SEP, we prove that our system can achieve a diversity order equals to the number of antennas times the number of states.
- We provide a comprehensive comparison of the high SNR error performance of reconfigurable antennas with that of the generalized selection combining (GSC). We show that both systems achieve the same diversity order. Based on a comparison of array gains we also show that the error probability performance of the two systems is comparable.
- Finally, we discuss applicability of reconfigurable antennas in novel large antenna arrays and distributed antenna systems. Through extensive numerical examples, we illustrate how reconfigurable antennas achieve a good compromise between system performance and the required number of RF chains

The rest of the paper is organized as follows. In Section II we present the system model. The derivation of the MGF of the received SNR is presented in Section III followed by the performance analysis in Section IV. In Section V the analysis is extended to consider correlated channels. The comparison with the GSC is presented in Section VI. Applications of reconfigurable antennas in novel wireless networks is discussed in Section VII, followed by concluding remarks in Section VIII.

II. System Model

We consider a system model with one transmitter and N receivers. Each receiver has a reconfigurable antenna with S reconfigurable states. Thus, the complete channel vector for the system can be written as $\mathbf{h}_c \in \mathcal{C}^{NS\times 1}$, with independent and identically distributed entries. Considering Rayleigh fading we assume these entries to be zero mean, unit variance,[1] circularly symmetric Gaussian random variables. In reconfigurable systems, each receiver selects the best state from all reconfigurable states, according to some desired performance metric. In this paper, we select state j at antenna n such that

$$j = \arg\ \max_k |h_{nk}|^2, \tag{1}$$

where h_{nk} is the channel between the transmitter and the k-th state of antenna n. Similar to [24], we assume the coherence time of the channel is long such that a large number of bits can be transmitted within this time. Since h_{nk} is Gaussian distributed with $h_{nk} \sim \mathcal{CN}(0,1)$, $|h_{nk}|^2$ has an exponential distribution with rate parameter one, and $|h_{nj}|^2$ is the maximum of S such independent and identical random variables.

[1]Note that, the channel powers may change between states depending on how reconfigurability is achieved. In this paper, we take a general approach without focusing on one specific reconfigurable mechanism. As such, we assume the channel powers to remain constant between different states.

After selecting the states for all the antennas at the receiver, we can write the $\mathcal{C}^{N\times 1}$ received vector as

$$\mathbf{y} = \mathbf{h}s + \mathbf{n}, \tag{2}$$

where s denotes the transmitted symbol and $\mathbf{h}$ denotes the $\mathcal{C}^{N\times 1}$ selected channel vector. The variable $\mathbf{n}$ denotes the $\mathcal{C}^{N\times 1}$ additive white Gaussian noise vector at the receive antennas which has independent entries with variance σ^2. At the receiver, we apply MRC to estimate the transmitted symbols. Based on (2), the output of the combiner is given by [26]

$$\tilde{\mathbf{y}} = s + \frac{\mathbf{h}^H\mathbf{n}}{\mathbf{h}^H\mathbf{h}}. \tag{3}$$

As such, the instantaneous SNR at the receiver can be written as

$$\gamma = \rho Z, \tag{4}$$

where $Z = \sum_{n=1}^{N} |h_{nj}|^2$ and $\rho = \frac{E\{|s|^2\}}{\sigma^2}$. We note that the instantaneous received SNR of a $N \times 1$ multiple-input single-output (MISO) system where the transmitter side employs a reconfigurable antenna array takes the same form as (4) when maximal ratio transmission (MRT) is employed. Thus, the following analysis directly applies to a MISO system as well.

III. Moment Generating Function

In this section, we derive a new closed-form expression for the MGF of the instantaneous received SNR in a reconfigurable antenna array system. We denote the maximum channel gain at antenna n by

$$x_{nj} = \max_k |h_{nk}|^2 = |h_{nj}|^2, \tag{5}$$

Based on (4) and (5), the MGF of γ can be written as

$$\mathcal{M}_\gamma(t) = E\{e^{t\gamma}\} = \prod_{j=1}^{N} E\{e^{t\rho x_{nj}}\}, \tag{6}$$

where the expectation in (6) is taken over the channel fading. Note that the problem of finding the MGF of γ has now reduced to finding the MGF of x_{nj}. Based on the order statistics, it is straightforward to write the CDF expression of the maximum of S exponentials as

$$F_{x_{nj}}(x) = (1 - e^{-x})^S. \tag{7}$$

Based on (7), the MGF of x_{nj} can be written as

$$M_{x_{nj}}(t\rho) = S\int_0^\infty e^{(t\rho-1)x}(1 - e^{-x})^{S-1}dx, \tag{8}$$

which can be solved by re-expressing $(1-e^{-x})^{S-1}$ in (8) as a summation based on the binomial expansion and solving the resultant integral using [27, eq. (3.310)] as

$$M_{x_{nj}}(t\rho) = S\sum_{r=0}^{S-1}\binom{S-1}{r}\frac{(-1)^r}{1+r-t\rho}, \quad \text{for } t\rho < 1 + r. \tag{9}$$

Since $M_{x_{nj}}(t\rho) = E\{e^{t\rho x_{nj}}\}$ we substitute (9) into (6) to find an exact expression for $\mathcal{M}_\gamma(t)$ as

$$\mathcal{M}_\gamma(t) = \left[S\sum_{r=0}^{S-1}\binom{S-1}{r}\frac{(-1)^r}{1+r-t\rho}\right]^N. \tag{10}$$

This closed-form expression provides a unified result to accurately analyse the performance of a reconfigurable antenna array system. We also note that the result in (10) generalizes the MGF results for conventional SC and MRC. In particular, for the specific case of $N = 1$ (i.e., conventional SC) it is straightforward to see that (10) reduces to the classical result $\mathcal{M}_\gamma^{SC}(t) = S\sum_{r=0}^{S-1}\binom{S-1}{r}\frac{(-1)^r}{1+r-t\rho}$. Similarly, for the particular case of $S = 1$ (i.e., conventional MRC), it is easy to see that (10) reduces to the well-known result $\mathcal{M}_\gamma^{MRC}(t) = \left(\frac{1}{1-t\rho}\right)^N$ [28].

Next, we proceed by re-expressing the MGF in (10) to allow easy integration as

$$\mathcal{M}_\gamma(t) = \left[\frac{S!}{\prod_{q=0}^{S-1}(1+q-t\rho)}\right]^N, \tag{11}$$

where we substitute

$$\sum_{r=0}^{S}\binom{S-1}{r}\frac{(-1)^r}{r+1-t\rho} = \frac{(S-1)!}{\prod_{q=0}^{S-1}(q+1-t\rho)}, \tag{12}$$

which is proven in Appendix A. This result can be used to derive the PDF of γ as [26]

$$f_\gamma(x) = \frac{1}{2\pi}\int_{-\infty}^{\infty}\sum_{q=0}^{S-1}\sum_{n=1}^{N}\frac{a_{nq}}{(1+q-t\rho)^n}e^{-jtx}dt, \tag{13}$$

where (13) is obtained using a partial fraction decomposition with a_{nq} denoting the coefficient corresponding to the nq-th fraction. These coefficients can be computed algebraically for any special case using the set of formulas in [27, eq. (2.101)]. Based on the integral identity in [27, eq. (3.382, 7)], the final expression for the PDF of γ can be derived as

$$f_\gamma(x) = \sum_{q=0}^{S-1}\sum_{n=1}^{N}a_{nq}\frac{x^{n-1}e^{-x/\eta}}{(1+q)^n(n-1)!\eta^n}, \tag{14}$$

where $\eta = \frac{\rho}{1+q}$. Similarly, an exact expression for the CDF of γ can be derived as

$$F_\gamma(x) = \sum_{q=0}^{S-1}\sum_{n=1}^{N}a_{nq}\frac{\Gamma(n, x/\eta)}{(1+q)^n(n-1)!}, \tag{15}$$

where Γ denotes the lower incomplete gamma function. In Section IV, we use the PDF and CDF expressions in (14) and (15) to derive expressions for important performance measures in a SIMO system with reconfigurable antenna arrays.

IV. Performance Analysis

In this section, we derive novel closed-form expressions for important performance measures in reconfigurable antenna array systems based on the SNR distributions derived in Section III. We introduce the notation $(N : S)$ to denote the

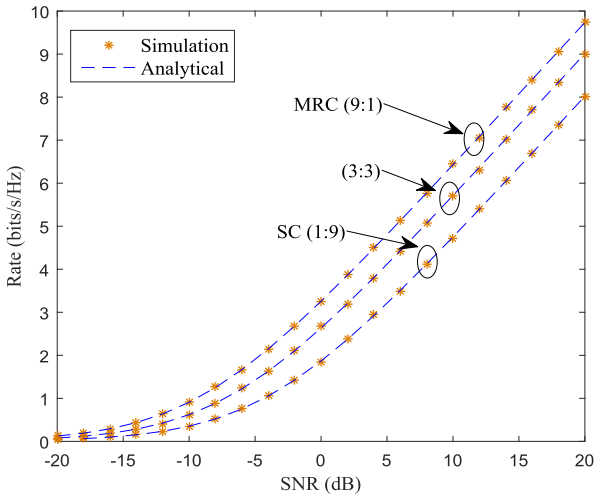

Fig. 1. The achievable rate versus the average received SNR for (9 : 1), (3 : 3) and (1 : 9) systems.

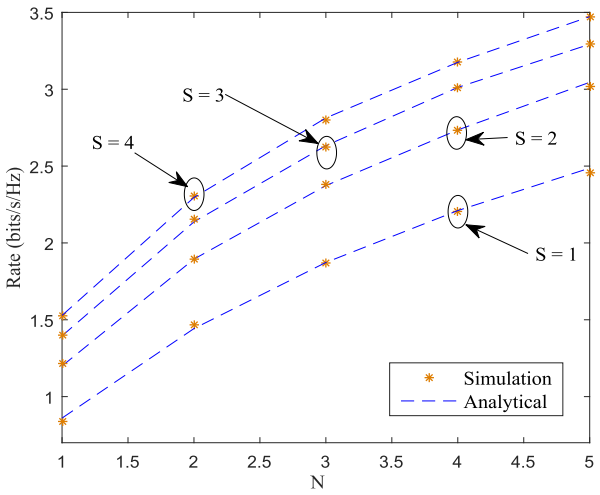

Fig. 2. The achievable rate versus the number of antennas, N, for different numbers of reconfigurable states, S.

dimension of a reconfigurable system with N antennas with S reconfigurable states each. This notation shall be utilized throughout.

A. Achievable Rate

The achievable rate of the transmitter in this system can be written as

$$R = \int_0^\infty \log_2(1+x) f_\gamma(x) dx. \tag{16}$$

Substituting (14) into (16) and following standard mathematical manipulations in [29] we can derive an easy to evaluate expression for the achievable rate as

$$R = \log_2 e \sum_{q=0}^{S-1} \sum_{n=1}^{N} \frac{e^{1/\eta} a_{nq} (1+q)^{-n}}{(n-1)! \eta^n} [\Theta + \Lambda], \tag{17}$$

where

$$\Theta = \sum_{k=0}^{n-1} \frac{(n-1)!(-1)^{n-k-1} \eta^{k+1}}{(n-k-1)!} [E_1(1/\eta)], \tag{18}$$

with $E_1(1/\eta) = \int_{1/\eta}^\infty \frac{e^{-x}}{x} dx$ denoting the exponential integral function [27], and

$$\Lambda = \sum_{k=0}^{n-1} \frac{(n-1)!(-1)^{n-k-1} \eta^{k+1}}{(n-k-1)!} \left[\sum_{z=1}^{k} \frac{e^{-(1/\eta)}}{z} \sum_{l=0}^{z-1} \frac{1}{\eta^l l!} \right]. \tag{19}$$

Since the exponential integral function is a well-known function that is built-in to many mathematical tools, the calculation in (17) is much faster and more precise as compared to numerical integration. Thus, it provides a much more computationally efficient solution to derive achievable rate results in a SIMO system with reconfigurable antenna arrays.

Example 1: In Fig. 1, we plot the achievable rate of the transmitter versus the average received SNR for a three antenna system with three reconfigurable states each, i.e. $(N : S) = (3 : 3)$. We compare the performance of the $(3 : 3)$ system with two other special cases of size $(9 : 1)$ and $(1 : 9)$. The analytical results are generated using (17) and the simulation points are obtained using Monte Carlo simulations with channel fading and noise components for each simulation trial drawn from independent complex Gaussian distributions. The figure highlights the accuracy of our achievable rate expression. Note that a $(9 : 1)$ system is the conventional MRC with single state antennas while a $(1 : 9)$ system is the conventional SC, both with system dimensions comparable to the $(3 : 3)$ reconfigurable system. We observe that the achievable rate performance of a $(9 : 1)$ MRC system is better than that of the $(3 : 3)$ reconfigurable system. However, a $(9 : 1)$ MRC system requires three times more RF chains compared to the $(3 : 3)$ reconfigurable system to achieve this performance gain. As expected, the achievable rate performance of a $(3 : 3)$ reconfigurable system is better than that of the $(1 : 9)$ SC system.

Example 2: In Fig. 2, we plot the achievable rate versus N, for various values of S. We fix the transmit SNR at 0 dB and change S from one to four. The results show that for a fixed N, diminishing performance gains are obtained as the number of states increases. Furthermore, for a fixed S a nonnegligible performance gain can be obtained by increasing N, but the percentage of improvement diminishes with increasing N.

B. Symbol Error Probability

For many modulations, the SEPs can be constructed from a function of the form [30], [31]

$$P_e = E\{\phi Q(\sqrt{\beta\gamma})\} = \int_0^\infty \phi Q(\sqrt{\beta x}) f_\gamma(x) dx, \tag{20}$$

where $Q(.)$ denotes the Gaussian Q-function and (ϕ, β) are two parameters that change with the modulation M. Substituting (14) into (20), P_e can be solved as

$$P_e = \phi \sum_{q=0}^{S-1} \sum_{n=1}^{N} a_{nq} (1+q)^{-n} \left(\frac{1-\mu}{2}\right)^n \times \sum_{k=0}^{n-1} \binom{n-1+k}{k} \left(\frac{1+\mu}{2}\right)^k, \tag{21}$$

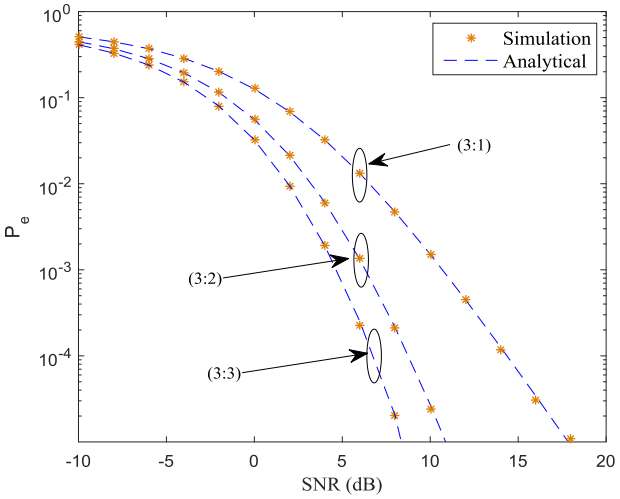

Fig. 3. The symbol error probability versus the average received SNR for $N = 3$ antennas.

where $\mu = \sqrt{\frac{\eta\beta}{\eta\beta+2}}$. The result in (21) is obtained by re-expressing the Gaussian Q-function in (20) in-terms of the complimentary error function, *erfc(.)* and solving the resultant integral using the identity in [26, p. 781]. This closed-form expression provides a computationally efficient solution to derive the SEP results for many modulations.

For M-ary quadrature amplitude modulation (MQAM), first order SEP approximations can be found via expressions of the form in (20). The exact SEP involve $E\{\phi Q(\sqrt{\beta\gamma})\}$ and $E\{\phi Q^2(\sqrt{\beta\gamma})\}$ [32, eq. (20)] and the expectation over $Q^2(.)$ can be derived as

$$E\{\phi Q^2(\sqrt{\beta\gamma})\} = \phi \sum_{q=0}^{S-1}\sum_{n=1}^{N} \frac{a_{nq}(1+q)^{-n}}{4(n-1)!\eta^n} \times \left(\frac{(n-1)!}{\upsilon^n} - \frac{4}{\sqrt{\pi}\upsilon^n}\sum_{k=0}^{n-1}\frac{(n-1)!\upsilon^k}{k!}\Psi\right), \tag{22}$$

where $\upsilon = \frac{2}{\beta\eta}$, $\Psi = \frac{k!}{(2k-1)\sqrt{\pi}}\,{}_2\mathcal{F}_1\left(\frac{1}{2}+k, 1+k; \frac{3}{2}+k; -\nu\right)$ with ${}_2\mathcal{F}_1$ representing the hypergeometric function and $\nu = \frac{2+\beta\eta}{\beta\eta}$. The result in (22) is obtained by re-expressing the Gaussian Q-function in-terms of the complimentary error function, *erfc*(.) and solving the resultant integral using the identity in [33, eq. (17)]. The exact SEPs for M-ary phase shift keying (MPSK) and MQAM modulations are computable using (21) and (22), providing computationally efficient closed-form solutions. Note that this standard approach in deriving the SEP is widely used in literature [30], [34], [35], but to the best of our knowledge this is the first time it has been applied to reconfigurable antenna arrays. We also note that our SEP results in (21) together with (22) generalize the MPSK SEP results in [36, eq. (21)] when $S = 1$ and those in [36, eq. (26)] when $N = 1$ for conventional MRC and SC, respectively. Furthermore, our SEP results generalize the MQAM SEP results in [33] and [37] for conventional MRC and SC.

Example 3: In Fig. 3, we plot the SEP versus the average received SNR for Quadrature Phase Shift Keying (QPSK). We consider a three antenna system with $S = 1, 2$ and 3. The analytical results are generated using (21) and (22) as the exact SEP for QPSK is given by $E\{2Q(\sqrt{\gamma})\} - E\{Q^2(\sqrt{\gamma})\}$. The figure highlights the accuracy of our error probability expression and we observe that, increasing the number of states improves the error performance. At 8 dB received SNR, we achieve a 20-fold reduction in the SEP when the number of states increases from one to two. However, this reduces to a 10-fold improvement in the SEP when the number of states increases from two to three.

C. Outage Probability

The outage probability P_{out} is defined as the probability that the received SNR falls below a certain predetermined threshold SNR given by γ_{th} [4] and hence can be written as

$$P_{out} = P[\gamma < \gamma_{th}] = F_\gamma(\gamma_{th}). \tag{23}$$

The probability in (23) can be directly obtained using the CDF expression in (15) as

$$P_{out} = \sum_{q=0}^{S-1}\sum_{n=1}^{N} \frac{a_{nq}(1+q)^{-n}}{(n-1)!\eta^n}\left[\eta^n(n-1)! - e^{-\frac{\gamma_{th}}{\eta}} \times \sum_{k=0}^{n-1}\frac{(n-1)!\eta^{n-k}\gamma_{th}^k}{k!}\right]. \tag{24}$$

This closed-form expression provides a computationally efficient solution to derive the outage probability in a SIMO system with reconfigurable antennas. As a check, when the number of reconfigurable states at each antenna is one, i.e., $S = 1$, (24) reduces to

$$P_{out} = \sum_{n=1}^{N} a_{n1}\left[1 - e^{-\frac{\gamma_{th}}{\rho}}\sum_{k=0}^{n-1}\left(\frac{\gamma_{th}}{\rho}\right)^k\frac{1}{k!}\right]. \tag{25}$$

We also note that the coefficients in the partial fraction decomposition are all zeros, except for $n = N$, i.e., $a_{11} = a_{21} = \ldots = a_{(N-1)1} = 0$ and $a_{N1} = 1$. As such, the expression in (25) reduces to

$$P_{out} = 1 - e^{-\frac{\gamma_{th}}{\rho}}\sum_{k=0}^{N-1}\left(\frac{\gamma_{th}}{\rho}\right)^k\frac{1}{k!}, \tag{26}$$

which agrees with the previously known results for the outage probability for MRC in [28, p. 329, eq. (6.69)]. Furthermore, when the number antennas in the system is one, i.e., $N = 1$, (24) reduces to

$$P_{out} = \sum_{q=0}^{S-1} a_{1q}\left[\frac{1-e^{-\frac{\gamma_{th}}{\eta}}}{(1+q)}\right]. \tag{27}$$

Referring to the partial fraction decomposition in (13) we note that, when $N = 1$, the roots in the denominator polynomial are distinct. As such, the coefficients of the partial fraction decomposition can be derived as

$$a_{1q} = \frac{S!(-1)^q}{(S-1-q)!q!}. \tag{28}$$

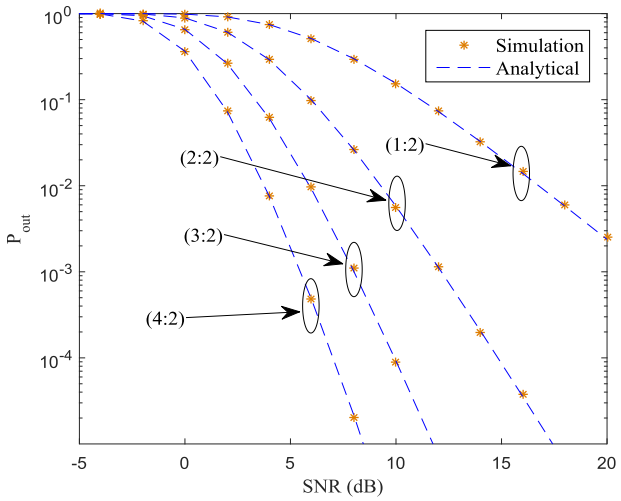

Fig. 4. The outage probability versus the average received SNR for $S = 2$ reconfigurable states.

Substituting (28) into (27) we get

$$P_{out} = \sum_{q=0}^{S-1} \frac{S!(-1)^q}{(S-1-q)!q!} \left[\frac{1 - e^{-\frac{\gamma_{th}}{\eta}}}{(1+q)} \right], \tag{29}$$

which agrees with the previously known results for SC in [4, eq. (26)].

Example 4: In Fig. 4, we plot the outage probability of the transmitter versus the average received SNR. The number of reconfigurable states in each antenna is fixed to two and we plot the outage performance for $(1:2), (2:2), (3:2)$ and $(4:2)$ systems. The SNR threshold is set to $\gamma_{th} = 7$ dB, such that all four systems of interest experience realistic outage probabilities. The analytical expressions are generated using our results in (24). We observe that our analytical results accurately follow the simulation points in all four cases. We also observe that, increasing the number of states improves the outage probability, but similar to the error probability the rate of improvement decreases with the increasing number of states.

D. Extension to Non-Identical Channels

We would like to highlight that the same approach in Section III can be used to derive the SNR distributions of a reconfigurable system when receivers experience independent but non-identical channels with distinct channel gains. This is particularly interesting as it allows the reconfigurable antennas to be located at geographically separated locations creating a macro-diversity scenario. Non-identical channels would be generated as a result of the large scale fading gains, i.e., distance dependent path loss and shadowing, experienced by different paths.

Different from (7), the CDF expression for the non-identical case can be written as

$$F_{x_{nj}}(x) = (1 - e^{-\lambda_n x})^S, \tag{30}$$

where $\lambda_n = 1/g_n^2$ with g_n^2 representing the large-scale fading gain[2] between the transmitter and receiver n. Based on (30), the MGF of γ in (6) results in

$$\mathcal{M}_\gamma(t) = \prod_{n=1}^{N} \left[\frac{S!\lambda_n^S}{\prod_{q=0}^{S-1}(\lambda_n(1+q) - t\rho)} \right]. \tag{31}$$

In the following we consider a special case of fully distributed antennas with distinct large-scale fading gains, i.e, $\lambda_n \neq \lambda_l$ for $n \neq l$. For such a network the PDF and the CDF of γ can be derived following the same steps as in Section III to obtain

$$f_\gamma(x) = \sum_{q=0}^{S-1}\sum_{n=1}^{N} \frac{e^{-x/\eta_n} \prod_{l=1}^{N} S!\lambda_l^S}{\eta_n \lambda_n (1+q) \prod_{l=1, l\neq n, r\neq q}^{N} (\lambda_l(1+r) - \lambda_n(1+q))}, \tag{32}$$

$$F_\gamma(x) = \sum_{q=0}^{S-1}\sum_{n=1}^{N} \frac{\Gamma(1, x/\eta_n) \prod_{l=1}^{N} S!\lambda_l^S}{\lambda_n (1+q) \prod_{l=1, l\neq n, r\neq q}^{N} (\lambda_l(1+r) - \lambda_n(1+q))}, \tag{33}$$

where $\eta_n = \frac{\rho}{\lambda_n(1+q)}$. Note that, the result in (32) and (33) follow directly from (13) and (15), respectively. Based on the MGF, PDF and CDF expressions of γ the performance of a fully distributed system with reconfigurable antennas can be well analysed. For the sake of completion, we have included the achievable rate and the SEP expressions as follows.

Using Section IV-A, the exact closed-form expression for the achievable rate of the transmitter can be derived as

$$R = \log_2(e) \sum_{q=0}^{S-1}\sum_{n=1}^{N} \frac{\omega_{nq} e^{-1/\eta_n} E_1(1/\eta_n)}{\lambda_n(1+q)}. \tag{34}$$

where $\omega_{nq} = \frac{\prod_{l=1}^{N} S!\lambda_l^S}{\prod_{l=1, l\neq n, r\neq q}^{N} (\lambda_l(1+r) - \lambda_n(1+q))}$. Substituting the MGF expression in (31) into [32, eq. (9.15)], the SEP of the transmitter with MPSK modulation can be derived as

$$P_e = \frac{1}{\pi} \sum_{q=0}^{S-1}\sum_{n=1}^{N} \frac{\omega_{nq}}{\lambda_n(1+q)} \left[\epsilon - \frac{\tan^{-1}\left(\beta_{nq} \tan\epsilon\right)}{\beta_{nq}} \right], \tag{35}$$

where $\epsilon = (M-1)\pi/M$ and $\beta_{nq} = \sqrt{(\varrho\rho + \lambda_n(1+q))/(\varrho\rho)}$ with $\varrho = \sin^2\frac{\pi}{M}$. Whilst not shown here, the derivation of the SEP expression for MQAM follows easily from [32, eq. (9.21)].

Example 5: In Fig. 5, we consider a circular cell of radius $R = 1$ km. The central processor which is located at the cell center receives signals from three distributed reconfigurable antennas, located in equal distances from the cell center. The location of the transmitter is illustrated by 'x' in the figure. We assume that the channels are subject to Rayleigh fading and distance dependent path loss with path loss exponent $\alpha = 4$. Fig. 6 illustrates the simulated and the analytical bit error probability (BEP) results for binary phase shift keying (BPSK) modulation. Similar to Fig. 3, we plot the performance for (3:1), (3:2) and (3:3) systems. The three distributed sites located at A, B and C in Fig. 5 are equipped with a single RF chain each. We observe that the analytical expressions, generated using (35), accurately follow the simulation results.

[2]The path loss experienced by each antenna at a given receiver site is identical as the cluster of S antennas are co-located.

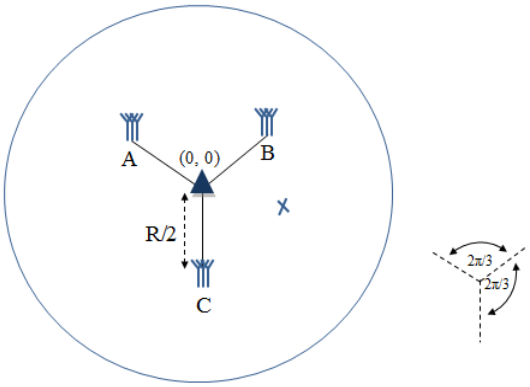

Fig. 5. A circular area with radius $R = 1$ km. Three distributed reconfigurable antennas located in $R/2$ distances from the centre are connected to the central processor at the centre (location 0,0). The transmitter is located at 'x' (location 220,-100).

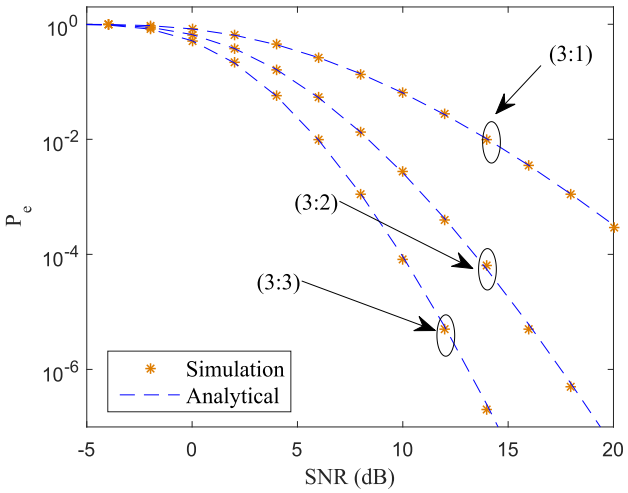

Fig. 6. The bit error probability versus the average received SNR for distributed reconfigurable antennas.

As expected the bit error probability decreases with an increasing number of states.

V. Asymptotic Analysis With Correlated States

In this section, we consider a more general case in which the channels experienced by different reconfigurable states within each antenna are correlated. This is particularly interesting as the reconfigurable states, which are realized based on the radiation pattern characteristics, are likely to be correlated within each antenna array [13]. In this paper, we assume the correlation between states is denoted by a coefficient τ which would change depending on how the reconfigurability is defined. Unlike the independent case, deriving the exact expressions for the PDF and the CDF of x_{nj} is quite complicated in the correlated case even with a small number of correlated states. The joint PDF of the channels experienced by correlated states also takes a very complicated form. In the simplest possible case, where each antenna has one state, we have an exponential distribution (the square of the Rayleigh channel gain). In the case with two reconfigurable states, we obtain a pair of correlated exponentials that has a bivariate exponential distribution with a PDF containing a Bessel function [38]. In the case with three reconfigurable states, the joint PDF of three correlated exponentials is an infinite sum of products of Bessel functions [39]. As such, the exact analysis quickly become intractable.

Therefore, we proceed to analyse the high SNR behavior which accurately characterizes the diversity order and the array gain of a correlated system. The multivariate PDF of S correlated exponentials $x_1, x_2, \ldots, x_S$ is well known and can be found in [40, eq. (24)]. For the sake of completeness we have given the multivariate PDF in (36), shown at the bottom of this page, where $\bar{X} = X_1, X_2, \ldots, X_S$ and the $S \times S$ matrix Θ is an inverse correlation matrix given by, $\Theta = E[\mathcal{R}\{\mathbf{h}_n\}\mathcal{R}\{\mathbf{h}_n^*\}]^{-1}$ with $\mathcal{R}\{\mathbf{h}_n\}$ denoting the $S \times 1$ vector containing the real part of the channels between the transmitter and antenna n. The term Θ_{sv} denotes the (s, v)-th element of Θ. When the reconfigurable states are uncorrelated, i.e., independent channels, Θ reduces to $2\mathbf{I}$ with $\mathbf{I}$ denoting the identity matrix. Let the power series expansion of $f_{\bar{X}}(x_1, x_2, \ldots, x_S)$ be given by

$$f_{\bar{X}}(x_1, x_2, \ldots, x_S) = \sum_{i_1=0}^{\infty} \cdots \sum_{i_S=0}^{\infty} C_{i_1 i_2 \ldots i_S} \prod_{k=1}^{S} x_k^{i_k}, \quad (37)$$

where $C_{i_1 i_2 \ldots i_S}$ is the coefficient of the $(i_1 i_2 \ldots i_S)$-th term. We can write an expression for the CDF of $x_1, x_2, \ldots, x_S$ by integrating (37) from zero to x_l, where $l = 1, 2 \ldots S$, which results in

$$F_{\bar{X}}(x_1, x_2, \ldots, x_S) = \sum_{i_1=0}^{\infty} \cdots \sum_{i_S=0}^{\infty} C_{i_1 i_2 \ldots i_S} \prod_{k=1}^{S} \left(\frac{x_k^{i_l+1}}{i_k + 1} \right). \quad (38)$$

Since x_{nj} is the maximum of $x_1, x_2, \ldots, x_S$, next we write the CDF of x_{nj} in terms of $F_{\bar{X}}(x_1, x_2, \ldots, x_S)$ as

$$F_{x_{nj}}(x) = P(x_{nj} < x) = F_{X_1, X_2, \ldots, X_S}(x, x, \ldots, x), \quad (39)$$

which, after substituting in (38), results in

$$F_{x_{nj}}(x) = \sum_{i_1=0}^{\infty} \cdots \sum_{i_S=0}^{\infty} \Psi x^{\sum_{k=1}^{S} i_k + S}, \quad (40)$$

where $\Psi = \frac{C_{i_1 i_2 \ldots i_S}}{\prod_{k=1}^{S}(i_k+1)}$. Differentiating $F_{X_{nj}}(x)$ in terms of x, the PDF of x_{nj} can be derived as

$$f_{X_{nj}}(x) = \sum_{i_1=0}^{\infty} \cdots \sum_{i_S=0}^{\infty} \Psi \left(\sum_{k=1}^{S} i_k + S \right) x^{\sum_{k=1}^{S} i_k + S - 1}. \quad (41)$$

$$f_{\bar{X}}(x_1, x_2, \ldots, x_S) = \frac{|\Theta| e^{-\frac{1}{2}\sum_{s=1}^{S} \Theta_{ss} x_s}}{(4\pi)^S} \int_{-\pi}^{\pi} \cdots \int_{-\pi}^{\pi} \exp\left(- \sum_{s,v=1, s<v}^{S} \Theta_{sv} \sqrt{x_s x_v} \cos(\phi_s - \phi_v) \right) d\phi_1 \ldots d\phi_S, \quad (36)$$

Substituting (41) into (6), and subsequently solving the integral using the identity in [27, eq. (3.351, 3)] the MGF of x_{nj} can be re-expressed as

$$\mathcal{M}_{x_{nj}}(t\rho) = \sum_{i_1=0}^{\infty} \cdots \sum_{i_S=0}^{\infty} \frac{\Psi\left(\sum_{k=1}^{S} i_k + S\right)!}{(-t\rho)^{\sum_{k=1}^{S} i_k + S}}. \quad (42)$$

As such, we find the MGF of γ written in a series expansion by substituting (42) into (6) as

$$\mathcal{M}_{\gamma}(t) = \left[\sum_{i_1=0}^{\infty} \cdots \sum_{i_S=0}^{\infty} \frac{\Psi\left(\sum_{k=1}^{S} i_k + S\right)!}{(-t\rho)^{\sum_{k=1}^{S} i_k + S}} \right]^{N}. \quad (43)$$

Note that the value of ρ is large in the high SNR regime. According to [41, Proposition 03], the exact diversity order and the array gain can be found from the smallest order term in the MGF $\mathcal{M}_{\gamma}(t)$. Hence, we can ignore the higher order terms and find a high SNR approximation for the MGF $\mathcal{M}_{\gamma}(t)$ as

$$\mathcal{M}_{\gamma}(t) \simeq \left[\frac{C_{\bar{i}_1 \bar{i}_2 \ldots \bar{i}_S} \left(\sum_{k=1}^{S} \bar{i}_k + S\right)!}{(-t\rho)^{\sum_{k=1}^{S} \bar{i}_k + S} \prod_{k=1}^{S} (\bar{i}_k + 1)} \right]^{N}, \quad (44)$$

where $C_{\bar{i}_1 \bar{i}_2 \ldots \bar{i}_S}$ denotes the coefficient and $\bar{i}_1, \bar{i}_2, \ldots \bar{i}_S$ denote the powers of $x_1, x_2 \ldots x_S$, respectively, in the smallest order term in (37).

Next, we proceed to find $\bar{i}_1, \bar{i}_2, \ldots, \bar{i}_S$ and $C_{\bar{i}_1 \bar{i}_2 \ldots \bar{i}_S}$ based on (36). From the series representation of the exponential function in [27, eq. (1.211)], the smallest order term in (36) can be separated as

$$f_{\bar{X}}(x) = \frac{|\Theta|}{2^S} + o(x_1, x_2, \ldots, x_S), \quad (45)$$

where $o(x_1, x_2, \ldots, x_S)$ denotes the higher order terms of $x_1, x_2, \ldots, x_S$. Comparing (45) with (37), we find that $C_{\bar{i}_1 \bar{i}_2 \ldots \bar{i}_S} = \frac{|\Theta|}{2^S}$ and $\bar{i}_1 = \ldots \bar{i}_S = 0$. As such, the high SNR approximation of $\mathcal{M}_{\gamma}(t)$ can be derived as

$$\mathcal{M}_{\gamma}(t) \simeq \left[\frac{|\Theta| S!}{(-2t\rho)^S} \right]^{N}. \quad (46)$$

Substituting (46) into [32, eq. (9.15)], and solving the resultant integral using the identity in [27, eq. (2.513, 1)] we can derive an asymptotic bound on the error probability for MPSK modulation as

$$P_e^{asy} = \frac{1}{\pi} \left(\frac{|\Theta| S!}{(2\varrho\rho)^S} \right)^{N} \Delta, \quad (47)$$

where

$$\Delta = \frac{1}{2^{2NS}} \binom{2NS}{NS} \epsilon + \frac{(-1)^{NS}}{2^{2NS-1}} \sum_{k=0}^{NS-1} (-1)^k \binom{2NS}{k} \frac{\sin(2NS-2k)\epsilon}{2NS-2k}. \quad (48)$$

Comparing (48) with $P_e^{asy} = (\frac{G_a}{\rho})^{G_d}$ [41], where G_d is the diversity order and G_a is the array gain, our asymptotic bound reveals that our reconfigurable antenna array system with S correlated states can achieve a diversity order of NS and an array gain of

$$G_a = \frac{2\varrho \pi^{1/NS}}{(|\Theta| S!)^{1/S} \Delta^{1/NS}}. \quad (49)$$

Similarly, the asymptotic bounds for the error probability of M-QAM, can be derived using [32, eq. (9.21)] as

$$P_e^{asy} = \frac{4\Upsilon}{\pi} \left(1 - \frac{1}{\sqrt{M}}\right) \left(\frac{|\Theta| S!}{(2\varrho_{QAM}\rho)^S} \right)^{N}, \quad (50)$$

where

$$\Upsilon = \frac{\pi (2NS-1)!!}{2(2NS)!!} - \left(1 - \frac{1}{\sqrt{M}}\right) \left(\frac{\pi}{2^{2NS+2}} \binom{2NS}{NS} + \frac{(-1)^{NS}}{2^{2NS}} \sum_{k=0}^{NS-1} (-1)^k \binom{2NS}{k} \frac{\sin(NS-k)\pi/2}{NS-k} \right), \quad (51)$$

and $\varrho_{QAM} = 3/2(M-1)$. The expression in (50) is achieved using the integral identity in [27, eq. (2.513, 1)] and [27, eq. (3.621, 3)]. From (50), the exact diversity order and the array gain follows easily.

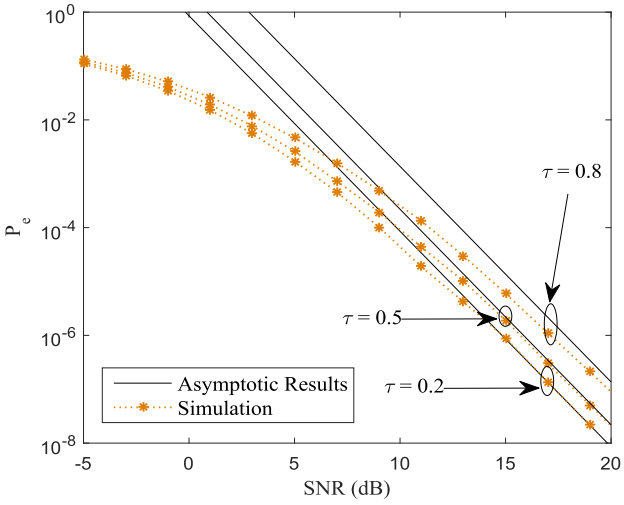

Fig. 7. The bit error probability versus the average received SNR for correlated channels

Example 6: In Fig. 7, we plot the BEP versus the average received SNR for BPSK modulation when the states of the reconfigurable system are correlated. We fix N and S to two and plot the results for three scenarios by changing the correlation coefficient, $\tau = 0.2, 0.5$ and 0.8. The correlated channel values are generated such that $h_{n1} = \tau h_{n2} + \sqrt{1-|\tau|^2}\kappa$ with h_{n2} and κ denoting independent and identical complex Gaussian random variables with zero mean and unit variance i.e., $h_{n2}, \kappa \sim \mathcal{CN}(0,1)$. We note that the asymptotic results generated using (48) accurately characterizes the diversity order of the simulation. Due to the effect of higher order terms in (45) it gets closer to the exact only at very high SNRs. When the correlation between states increases the BEP increases, while the diversity order remains constant at four.

VI. Comparison With Generalized Selection Combining

In this section, we compare the high SNR error probability performance of the current reconfigurable antenna array system with a traditional antenna selection scheme that uses GSC. In contrast to the reconfigurable system, in antenna selection with GSC, the receiver picks the set of antennas that experience the best channels out of all the receiving antennas. The reconfigurable system can therefore be viewed as a restricted version of antenna selection as discussed in Section I. In the following, we compare the two systems based on diversity order and array gain.

We consider an antenna selection scheme with GSC where the receiver picks the best L_c antennas out of L channels. When the channels are uncorrelated, the MGF expression for the received SNR is given in [4, eq. (12)]. We follow the same approach as above to derive an asymptotic bound for the SEP for BPSK as

$$P_{e_{GSC}}^{asy} = \frac{(2L-1)!!}{(2L)!!}\left[\frac{(L!)^{1/L}}{(L_c-1)!^{1/L}L_c^{(L-L_c+1)/L}2^{1/L}\rho}\right]^L, \tag{52}$$

where !! denotes the double factorial [27]. Thus, the diversity order of antenna selection with GSC is L and the array gain can be derived as

$$G_{a_{GSC}} = \frac{(2L)!!^{1/L}(L_c-1)!^{1/L}L_c^{(L-L_c+1)/L}2^{1/L}}{(2L-1)!!^{1/L}(L!)^{1/L}}. \tag{53}$$

In order to compare the two systems, we equate the system dimensions by setting $L = NS$ and $L_c = N$, which reveals that the diversity order of GSC equals the diversity order of the reconfigurable system. From (49), we can find the array gain for a reconfigurable antenna array system with uncorrelated states as

$$G_a = \frac{(2NS)!!^{1/NS}2^{\frac{1}{NS}}}{(2NS-1)!!^{1/NS}S!^{1/S}}. \tag{54}$$

Comparing the two array gains in (54) and (53) we can write,

$$\left[\frac{G_a}{G_{a_{GSC}}}\right]^{NS} = \frac{(NS)!}{(S!)^N(N-1)!N^{NS-N+1}}. \tag{55}$$

In Example 7 we use (55) to provide a comparison of the array gains for small systems of different sizes for both reconfigurable systems and antenna selection. Note that, when $N = 1$ and/or $S = 1$ antenna selection with GSC reduces to the reconfigurable system and we get

$$\left[\frac{G_a}{G_{a_{GSC}}}\right]^{NS} = 1. \tag{56}$$

Hence, $G_a = G_{a_{GSC}}$. When $N \geq 2$ and $S \geq 2$ we use the Stirling's approximation [42] and re-express the factorials in (55) to write

$$\left[\frac{G_a}{G_{a_{GSC}}}\right]^{NS} = \frac{N^{N-\frac{1}{2}}e^{N-1}}{(2\pi)^{\frac{N}{2}}(N-1)^{N-\frac{1}{2}}S^{\frac{(N-1)}{2}}}. \tag{57}$$

TABLE I
Ratio of Array Gains

$(N:S)$	$\left[\frac{G_a}{G_{a_{GSC}}}\right]$
(1:2), (2:1), (1:3), (3:1)	1
(2:2)	0.9306
(3:2)	0.9607
(2:3)	0.9247
(4:2)	0.8946
(2:4)	0.9273
(4:4)	0.8906

From (57), it is clear that $\left[\frac{G_a}{G_{a_{GSC}}}\right]^{NS}$ is a decreasing function of S. In Appendix B, we prove that $\left[\frac{G_a}{G_{a_{GSC}}}\right]^{NS}$ is a decreasing function of N as well. As such, we can write

$$\left[\frac{G_a}{G_{a_{GSC}}}\right]^{NS} \leq 1. \tag{58}$$

Therefore,

$$G_a \leq G_{a_{GSC}}. \tag{59}$$

This analytical derivation confirms that the antenna selection scheme with GSC outperforms the reconfigurable system. This however, is not surprising as GSC has more flexibility in selecting the best antennas out of all. This performance gain comes at a cost of an S-fold increase in the required number of physical antennas and sophisticated microwave switches. What interests us the most is *how different* the performance gain of the antenna selection scheme with GSC is compared to that of the reconfigurable system. We unravel that in the following.

For small values of N, the array gain ratio is tabulated in Table I. It provides a comparison of the array gains of reconfigurable systems and antenna selection, based on (55), for ten different system sizes considering BPSK modulation. Interestingly, we note that the ratio of array gains is closer to one for all small system configurations considered. Thus, despite the restriction of selecting the best out of a group of states the error performance of the reconfigurable system is very close to that of antenna selection. From Table I we also note that increasing N results in smaller array gain ratios. As such, we proceed to analyse how small the array gain ratio gets with increasing N.

We use (57) to analyze $\left[\frac{G_a}{G_{a_{GSC}}}\right]$ for large N as

$$\frac{G_a}{G_{a_{GSC}}} = \left[\frac{\left(\frac{N}{N-1}\right)^{1-\frac{1}{2N}}e^{1-\frac{1}{N}}}{(2\pi)^{\frac{1}{2}}S^{\frac{N-1}{2N}}}\right]^{\frac{1}{S}} \approx \left[\frac{e}{(2\pi S)^{1/2}}\right]^{1/S} \quad \text{for } N \gg 0, \tag{60}$$

where (60) is obtained by simply setting $N \to \infty$ in $\frac{G_a}{G_{a_{GSC}}}$. By equating the first derivative of (60) to zero we find that it has a critical point at $S = 3$. By straightforward mathematical manipulations, we also find that the second derivative of (60) is positive at that critical point. As such, $\frac{G_a}{G_{a_{GSC}}}$ reaches a

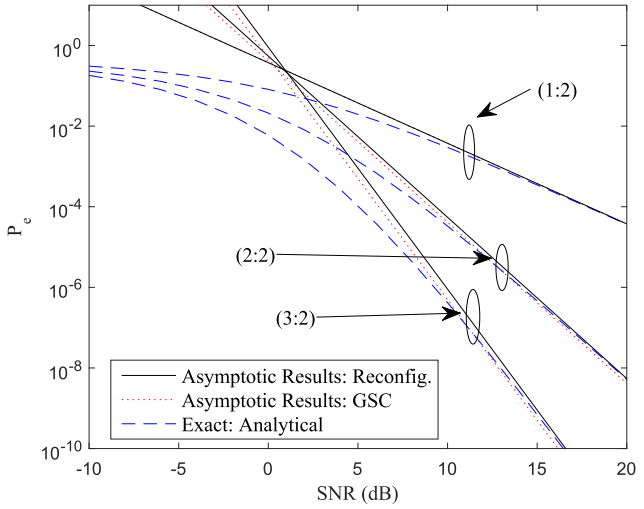

Fig. 8. The asymptotic error probability versus the average received SNR for the reconfigurable system and the antenna selection system with GSC.

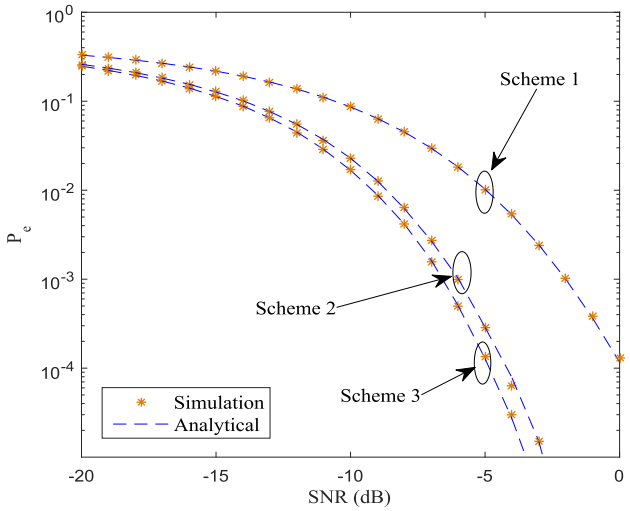

Fig. 9. The error probability versus the average received SNR for a large antenna arrays.

minimum of 0.855 at $S = 3$. Based on this observation we conclude that for large N

$$\frac{G_a}{G_{a_{GSC}}} \geq 0.855. \tag{61}$$

From (61) we learn that the two array gains are comparable even when when the antenna array is large. This small additional gain obtained through antenna selection comes at the cost of the added requirements of physical antennas and microwave switches, making reconfigurable antenna attractive.

Example 7: In Fig. 8, we compare the exact and the asymptotic error probability bounds for the reconfigurable system with that of antenna selection with GSC for BPSK modulation. For the reconfigurable system, the number of states in each antenna is fixed to two and we plot the performance for (1:2), (2:2) and (3:2) systems. For the antenna selection scheme, we equate the system dimensions by considering $(L, L_c) = (2, 1), (4, 2)$ and $(6, 3)$ systems. The exact error probability for reconfigurable systems are generated using (21), while the asymptotic results for the reconfigurable antenna system and the antenna selection scheme are generated using (48) and (52), respectively. The slope of the asymptotic bound confirms that a diversity order of NS can be achieved in both systems. As expected, the two asymptotic bounds coincide when $N = 1$. We observe in the figure that the performance of the antenna selection scheme with GSC is very close to that of the reconfigurable system, with the GSC performing slightly better. In fact, at 12 dB received SNR the $(3 : 2)$ reconfigurable system obtains an upper bound of $P_e = 5 \times 10^{-8}$ while the $(6, 3)$ antenna selection scheme with GSC obtains $P_e^{GSC} = 3 \times 10^{-8}$. Both probabilities are of the same order. However, we note that this small gain in GSC comes at a cost of three additional physical antennas and expensive microwave switches.

VII. Applications

In this section we present applications of our analytical results based on two novel concepts in wireless networks, namely large antenna arrays and distributed antenna systems.

A. Large Antenna Arrays

The massive multiple-input multiple-output (MIMO) paradigm, that uses large antenna arrays provides powerful means to achieve high data rates in future wireless networks [43]. While massive MIMO demands an order of magnitude more antennas, the deployment of that many RF chains at the base station site presents practical challenges. As discussed in Section I, the fabrication costs, signal processing complexity and power consumption limits the number of RF chains that can be deployed at a base station site. Several approaches, including the use of phase shifters and antenna selection, have been considered to limit the number of RF chains. In the following example we abstract out a MISO case from a MIMO network and illustrate how reconfigurable antennas can be used to unshackle these challenges.

Example 8: In this example we consider a massive MISO network with forty antennas at the base station transmitting to a single antenna receiver based on MRT beamforming. Fig. 9 plots the BEP versus the average received SNR for BPSK modulation. We assume that the base station is equipped with ten RF chains. We consider the three different schemes to select ten channels. In scheme 1, we consider random selection where the receiver picks ten antennas out of forty in random and connect the RF chains. Note that this is similar to a (10:1) reconfigurable antenna system. In scheme 2, we use ten reconfigurable antennas with four states each, i.e., (10:4) to virtually form forty antennas at the base station. In scheme 3, we consider generalized selection where the receiver picks the best ten antennas out of forty antennas. The analytical results for scheme 1 and 2 are generated using (21). The analytical results for scheme 2 was generated using [4, eq. (40)]. We observe that scheme 3 outperforms schemes 1 and 2. Interestingly, the gap between scheme 2 and 3 is very small making reconfigurable antennas a good candidate for the implementation of large antenna arrays, once hardware is considered.

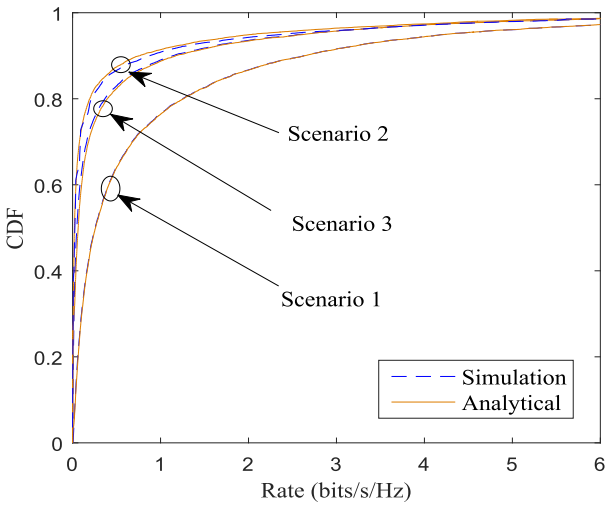

Fig. 10. The achievable rate CDF for the reconfigurable system with distributed antennas.

B. Distributed Antenna Systems

In recent years, DASs garnered much research attention due to their potential to improve the coverage and the capacity of wireless communications [44]. In DASs the antennas can be distributed at different locations within a cell or they can be extended across multiple cells via the emerging concept of base station cooperation. The processing is done at a central node which has access to the signals received at all distributed antennas. This was briefly discussed in Example 5 by considering a fixed set of transmitter and receiver locations. However, in a cellular environment the antennas can be scattered in random locations throughout the network. In the following example we compare the performance of a co-located antenna system and a DAS highlighting the use of reconfigurable antennas to implement partially distributed architectures.

Example 9: In Fig. 10, we analyze the achievable rate averaged over antenna locations. To do so, we consider the SIMO system in Example 5 and randomly place the antennas within the circular area in Fig. 5 to numerically generate the achievable rate CDF. In each iteration the antennas were uniformly distributed in random locations.[3] The transmit power is fixed such that the average received SNR at the central processor is 10 dB. In scenario 1, we consider a fully distributed network where nine single state antennas are distributed within the network. In scenario 2, we consider a fully co-located network where nine single state antennas are co-located. In scenario 3, we consider a partially distributed network where three $S = 3$ state reconfigurable antennas are distributed across the area. Note that scenario 1 and 2 require nine RF chains while scenario 3 requires only three RF chains. We observe that, despite the same number of RF chains required, scenario 1 outperforms scenario 2 highlighting the performance gains achieved with DASs. By comparing scenario 2 and 3, we note that the partially distributed network created using the reconfigurable antennas achieve a good compromise between system performance and the required number of RF chains in this example scenario.

[3]In cellular mobile networks, receiver sites are carefully planned to improve coverage. Selecting completely random locations for receiver sites represents an extreme case.

VIII. Conclusion and Future Work

In this paper, we considered a reconfigurable antenna array system where each receiver is equipped with reconfigurable antennas. Each antenna selects the best state depending on the channel between the transmitter and the receiver. Adopting a MRC receiver we derived new closed-form expressions for the MGF, PDF and CDF of the instantaneous received SNR. Based on these distributions we also derived expressions for important performance measurers of the transmitter. We extended our analysis to consider high SNR error performance when the reconfigurable states are correlated. The numerical examples presented illustrate the accuracy of our results and further highlight the performance difference between antenna selection and reconfigurable systems. Finally, we discuss the applicability of reconfigurable antennas in novel wireless networks. The conclusions of this paper can be easily generalized to the scenario with multiple transmitters where an orthogonal multiple access approach, such as orthogonal frequency division multiple access (OFDMA), is adopted. In the following, we outline several directions of interest for future extensions.

- An extension to Nakagami-m fading would allow performance over a more diverse range of channel conditions to be explored. While we realize that the exact analysis with Nakagami-m fading is mathematically challenging an approximation would be tractable. Similar to [3] with GSC, we would expect the gap between the performance of reconfigurable systems and conventional MRC to reduce as the severity of Nakagami-m fading increases.
- The analysis focused on the SIMO case. The results directly apply to the MISO case with MRT. It is desirable to extend this to a MIMO case with multiple antennas co-located both at the transmitter and the receiver. Note that this introduces a sum of channel gains in the state selection. As opposed to the exponential distribution in the current work, $|h_{nk}|$ will have a gamma distribution.
- Related to the above point, it would be desirable to introduce reconfigurability to the transmitter side also and analyse the performance of different state selection algorithms. The optimum state selection would perform an exhaustive search over the states of the reconfigurable antennas to maximize a given performance measure.

Appendix A
Proof of Equation (12)

Given two polynomials $P(x)$ and $R(x) = (x-\alpha_1)(x-\alpha_2)\dots(x-\alpha_l)$, the partial fraction decomposition of $P(x)/R(x)$ is given by [27]

$$\frac{P(x)}{R(x)} = \sum_{i=1}^{l} \frac{P(\alpha_i)}{R'(\alpha_i)(x-\alpha_i)}, \tag{62}$$

where R' denotes the derivative of the polynomial R. Let, $P(x) = (S-1)!$ and $R(x) = \prod_{q=0}^{S-1}(x+q+1)$,

such that $R'(x) = \sum_{u=0}^{S-1}\left[\prod_{q\neq u}^{S-1}(x+q+1)\right]$. Thus, from (62) we obtain

$$\frac{(S-1)!}{\prod_{q=0}^{S-1}(x+q+1)} = \sum_{i=1}^{S}\frac{(S-1)!}{(x+i)\sum_{u=0}^{S-1}\left[\prod_{q\neq u}^{S-1}(x+q+1)\right]}. \tag{63}$$

In order to simplify (63), we re-express the summation in the denominator to write

$$\frac{(S-1)!}{\prod_{q=0}^{S-1}(x+q+1)} = \sum_{i=1}^{S}\frac{(S-1)!}{(x+i)\prod_{q\neq i-1}^{S-1}(q-i+1)}. \tag{64}$$

Then, we note that the resulting product in the denominator can be further simplified as

$$\prod_{q\neq i-1}^{S-1}(q-i+1) = (-1)^{i-1}(i-1)!(S-i)!. \tag{65}$$

Substituting (65) into (64) we obtain

$$\begin{aligned}\frac{(S-1)!}{\prod_{q=0}^{S-1}(x+q+1)} &= \sum_{i=1}^{S}\frac{(S-1)!}{(x+i)(-1)^{i-1}(i-1)!(S-i)!}\\ &= \sum_{i=1}^{S}\binom{S-1}{i-1}\frac{(-1)^{i-1}}{x+i}.\end{aligned} \tag{66}$$

Comparing (66) with (10) we substitute $r = i-1$ and $x = -t\rho$ to write

$$\frac{(S-1)!}{\prod_{q=0}^{S-1}(q+1-t\rho)} = \sum_{r=0}^{S}\binom{S-1}{r}\frac{(-1)^{r}}{r+1-t\rho}. \tag{67}$$

APPENDIX B
PROOF OF EQUATION (58)

In the following, we analyse (57) with respect to the variable N. Let,

$$\left[\frac{G_a}{G_a^{GSC}}\right]^{NS} = \Upsilon(N) = \frac{N^{N-\frac{1}{2}}e^{N-1}}{(N-1)^{N-\frac{1}{2}}(2\pi)^{\frac{N}{2}}S^{\frac{(N-1)}{2}}}. \tag{68}$$

In order to prove that $\Upsilon(N)$ is a decreasing function of N, we first consider

$$\begin{aligned}\Upsilon(N+1)-\Upsilon(N) = &\frac{(N+1)^{N+\frac{1}{2}}e^{N}}{(N)^{N+\frac{1}{2}}(2\pi)^{\frac{N+1}{2}}S^{\frac{N}{2}}}\\ &-\frac{N^{N-\frac{1}{2}}e^{N-1}}{(N-1)^{N-\frac{1}{2}}(2\pi)^{\frac{N}{2}}S^{\frac{(N-1)}{2}}}.\end{aligned} \tag{69}$$

If (69) is less than or equal to zero, then $\Upsilon(N)$ is a decreasing function of N. Let us assume that

$$\Upsilon(N+1)-\Upsilon(N) \leq 0, \tag{70}$$

and in the following, we prove that this assumption is in fact true. Substituting (69) into (70) we obtain

$$\begin{aligned}\frac{(N+1)^{N+\frac{1}{2}}e^{N}}{(N)^{N+\frac{1}{2}}(2\pi)^{\frac{N+1}{2}}S^{\frac{N}{2}}} &\leq \frac{N^{N-\frac{1}{2}}e^{N-1}}{(N-1)^{N-\frac{1}{2}}(2\pi)^{\frac{N}{2}}S^{\frac{(N-1)}{2}}}\\ \frac{(N+1)^{N+\frac{1}{2}}(N-1)^{N-\frac{1}{2}}}{N^{2N}} &\leq \frac{(2\pi)^{\frac{N+1-N}{2}}S^{\frac{(N-N+1)}{2}}}{e^{N-N+1}}\\ \left(\frac{N^2-N}{N^2}\right)^{N}\sqrt{\frac{N+1}{N-1}} &\leq \frac{\sqrt{2\pi S}}{e}.\end{aligned} \tag{71}$$

The expression on the left hand side of (71) is an increasing function of N, which goes to one as N goes to infinity. As such,

$$\left(\frac{N^2-N}{N^2}\right)^{N}\sqrt{\frac{N+1}{N-1}} \leq 1. \tag{72}$$

We also note that

$$\frac{\sqrt{2\pi S}}{e} \geq 1, \quad \forall S \geq 1. \tag{73}$$

From (72) and (73) we obtain

$$\left(\frac{N^2-N}{N^2}\right)^{N}\sqrt{\frac{N+1}{N-1}} \leq 1 \leq \frac{\sqrt{2\pi S}}{e}. \tag{74}$$

Thus, the assumption in (70) is true and $\left[\frac{G_a}{G_a^{GSC}}\right]^{NS}$ is a decreasing function of N.

REFERENCES

[1] S. V. Hanly, I. B. Collings, Z. A. Shaikh, and P. Whiting, "Law of large numbers analysis of antenna selection aided downlink beamforming in massive MISO under RF chains constraint," in *Proc. Austral. Commun. Theory Workshop, AusCTW*, Melbourne, VIC, Australia, Jan. 2016, pp. 163–168.

[2] A. Mohammadi and F. M. Ghannouchi, "Single RF front-end MIMO transceivers," *IEEE Commun. Mag.*, vol. 49, no. 12, pp. 104–109, Dec. 2011.

[3] M. S. Alouini and M. K. Simon, "Performance of coherent receivers with hybrid SC/MRC over Nakagami-m fading channels," *IEEE Trans. Veh. Technol.*, vol. 48, no. 4, pp. 1155–1164, Jul. 1999.

[4] M. S. Alouini and M. K. Simon, "An MGF-based performance analysis of generalized selection combining over Rayleigh fading channels," *IEEE Trans. Commun.*, vol. 48, no. 3, pp. 401–415, Mar. 2000.

[5] D. A. Gore and A. J. Paulraj, "MIMO antenna subset selection with space-time coding," *IEEE Trans. Signal Process.*, vol. 50, no. 10, pp. 2580–2588, Oct. 2002.

[6] A. F. Molisch, M. Z. Win, Y.-S. Choi, and J. H. Winters, "Capacity of MIMO systems with antenna selection," *IEEE Trans. Wireless Commun.*, vol. 4, no. 4, pp. 1759–1772, Jul. 2005.

[7] X. Zhang and N. C. Beaulieu, "Performance analysis of generalized selection combining in generalized correlated nakagami-m fading," *IEEE Trans. Commun.*, vol. 54, no. 11, pp. 2103–2112, Nov. 2006.

[8] A. Dua, K. Medepalli, and A. J. Paulraj, "Receive antenna selection in MIMO systems using convex optimization," *IEEE Trans. Wireless Commun.*, vol. 5, no. 9, pp. 2353–2357, Sep. 2006.

[9] P. J. Smith, T. W. King, L. M. Garth, and M. Dohler, "A power scaling analysis of norm-based antenna selection techniques," *IEEE Trans. Wireless Commun.*, vol. 7, no. 8, pp. 3140–3149, Aug. 2008.

[10] M. D. Migliore, D. Pinchera, and F. Schettino, "Improving channel capacity using adaptive MIMO antennas," *IEEE Trans. Antennas Propag.*, vol. 54, no. 11, pp. 3481–3489, Nov. 2006.

[11] R. Bains, A. Kalis, and R. R. Muller, "On the link performance of a proposed compact antenna system," *IEEE Commun. Lett.*, vol. 12, no. 10, pp. 711–713, Oct. 2008.

[12] J. D. Boerman and J. T. Bernhard, "Performance study of pattern reconfigurable antennas in MIMO communication systems," *IEEE Trans. Antennas Propag.*, vol. 56, no. 1, pp. 231–236, Jan. 2008.

[13] V. Vakilian, J. F. Frigon, and S. Roy, "On the covariance matrix and capacity evaluation of reconfigurable antenna array systems," *IEEE Trans. Wireless Commun.*, vol. 13, no. 6, pp. 3452–3463, Jun. 2014.
[14] C. G. Christodoulou, S. A. L. Y. Tawk, and S. R. Erwin, "Reconfigurable antennas for wireless and space applications," *Proc. IEEE*, vol. 100, no. 7, pp. 2250–2261, Jul. 2012.
[15] A. Grau, M.-J. Lee, J. Romeu, H. Jafarkhani, L. Jofre, and F. D. Flaviis, "A multifunctional MEMS-reconfigurable pixel antenna for narrowband MIMO communications," in *Proc. IEEE Antennas Propag. Soc. Int. Symp.*, Honolulu, HI, USA, Jun. 2007, pp. 489–492.
[16] A. Grau, J. Romeu, M.-J. Lee, S. Blanch, L. Jofre, and F. D. Flaviis, "A dual-linearly-polarized MEMS-reconfigurable antenna for narrowband mimo communication systems," *IEEE Trans. Antennas Propag.*, vol. 58, no. 1, pp. 4–16, Jan. 2010.
[17] S. Nikalaou *et al.*, "Pattern and frequency reconfigurable annular slot using PIN diodes," *IEEE Trans. Antennas Propag.*, vol. 54, no. 2, pp. 439–448, Feb. 2006.
[18] S.-S. Oh, Y. Jung, Y. Ju, and H. Park, "Frequency-tunable open-ring microstrip antenna using varactor," in *Proc. Int. Conf. Electromagn. Adv. Appl.*, pp. 624–626, Sep. 2010.
[19] Y. Tawk, J. Costantine, S. E. Barbin, and C. G. Christodoulou, "Integrating laser diodes in a reconfigurable antenna system," in *Proc. SBMO/IEEE MTT-S Int. Microw. Optoelectron. Conf.*, Oct. 2011, pp. 794–796.
[20] S. J. Mazlouman, M. Soleimani, A. Mahanfar, C. Menon, and R. G. Vaughan, "Pattern reconfigurable square ring patch antenna actuated by hemispherical dielectric elastomer," *Electron. Lett.*, vol. 47, no. 3, pp. 164–165, Feb. 2011.
[21] P. Li, C. Zhang, and Y. Fang, "The capacity of wireless ad hoc networks using directional antennas," *IEEE Trans. Mobile Comput.*, vol. 10, no. 10, pp. 1374–1387, Oct. 2011.
[22] F. Babich and M. Comisso, "Multi-packet communication in heterogeneous wireless networks adopting spatial reuse: Capture analysis," *IEEE Trans. Wireless Commun.*, vol. 12, no. 10, pp. 5346–5359, Oct. 2013.
[23] A. Kalis, C. Papadias, and A. G. Kanatas, "ESPAR antenna for beamspace-MIMO systems using PSK modulation schemes," in *Proc. IEEE Int. Conf. Commun. (ICC)*, Glasgow, Scotland, U.K., Jun. 2007, pp. 5348–5353.
[24] P. J. Smith, A. Firag, P. A. Martin, and R. Murch, "SNR performance analysis of reconfigurable antennas," *IEEE Commun. Lett.*, vol. 16, no. 4, pp. 498–501, Apr. 2012.
[25] U. Afsheen, P. A. Martin, and P. J. Smith, "Space time state trellis codes for MIMO systems using reconfigurable antennas," *IEEE Trans. Commun.*, vol. 63, no. 10, pp. 3660–3670, Oct. 2015.
[26] J. G. Proakis, *Digital Communications*, 3rd ed. New York, NY, USA: McGraw-Hill, 1995.
[27] I. Gradshteyn and I. Ryzhik, *Table of Integrals, Series, and Products*, 7th ed. New York, NY, USA: Academic, 2007.
[28] T. S. Rappaport, *Wireless Communications: Principles and Practice*. Upper Saddle River, NJ, USA: Prentice-Hall, 1996.
[29] D. Torrieri, "Simple formulas for SIMO and MISO ergodic capacities," *Electron. Lett.*, vol. 47, no. 7, pp. 468–469, Mar. 2011.
[30] P. J. Smith, "Exact performance analysis of optimum combining with multiple interferers in flat Rayleigh fading," *IEEE Trans. Commun.*, vol. 55, no. 9, pp. 1674–1677, Sep. 2007.
[31] A. Goldsmith, *Wireless Communications*. New York, NY, USA: Cambridge Univ. Press, 2005.
[32] M. K. Simon and M.-S. Alouini, *Digital Communication Over Fading Channels*, 2nd ed. Hoboken, NJ, USA: Wiley, 2005.
[33] J. Lu, T. T. Tjhung, and C. C. Chai, "Error probability performance of L-branch diversity reception of MQAM in Rayleigh fading," *IEEE Trans. Commun.*, vol. 46, no. 2, pp. 179–181, Feb. 1998.
[34] A. Goldsmith, *Wireless Communications*, 4th ed. New York, NY, USA: McGraw-Hill, 2000.
[35] D. A. Basnayaka, P. J. Smith, and P. A. Martin, "The effect of macrodiversity on the performance of maximal ratio combining in flat Rayleigh fading," *IEEE Trans. Commun.*, vol. 61, no. 4, pp. 1384–1392, Apr. 2013.
[36] S. Chennakeshu and J. B. Anderson, "Error rates for Rayleigh fading multichannel reception of MPSK signals," *IEEE Trans. Commun.*, vol. 43, nos. 2–4, pp. 338–346, Feb. 1995.
[37] C.-J. Kim, Y.-S. Kim, G.-Y. Jeong, J.-K. Mun, and H.-J. Lee, "SER analysis of QAM with space diversity in Rayleigh fading channels," *ETRI J.*, vol. 17, no. 4, pp. 25–35, Jan. 1996.
[38] C. C. Tan and N. C. Beaulieu, "Infinite series representations of the bivariate Rayleigh and Nakagami-m distributions," *IEEE Trans. Commun.*, vol. 45, no. 10, pp. 1159–1161, Oct. 1997.
[39] M. Hagedorn, P. J. Smith, P. J. Bones, R. P. Millane, and D. Pairman, "A trivariate chi-squared distribution derived from the complex wishart distribution," *J. Multivariate Anal.*, vol. 97, no. 3, pp. 655–674, Mar. 2006.
[40] R. K. Mallik, "On multivariate Rayleigh and exponential distributions," *IEEE Trans. Inf. Theory*, vol. 49, no. 6, pp. 1499–1515, Jun. 2003.
[41] Z. Wang and G. B. Giannakis, "A simple and general parameterization quantifying performance in fading channels," *IEEE Trans. Commun.*, vol. 51, no. 8, pp. 1389–1398, Aug. 2003.
[42] M. Abramowitz and I. Stegun, *Handbook of Mathematical Functions*. Washington, DC, USA: Government Printing Office, 2002.
[43] T. L. Marzetta, "Noncooperative cellular wireless with unlimited numbers of base station antennas," *IEEE Trans. Wireless Commun.*, vol. 9, no. 11, pp. 3590–3600, Nov. 2010.
[44] R. Senanayake, P. L. Yeoh, and J. S. Evans, "Performance analysis of centralized and partially decentralized co-operative networks," *IEEE Trans. Commun.*, vol. 64, no. 2, pp. 863–875, Feb. 2016.

Rajitha Senanayake (S'11–M'16) received the B.E. degree in electrical and electronics engineering from the University of Peradeniya, Sri Lanka, and the B.IT degree in information technology from the University of Colombo, Sri Lanka, in 2009 and 2010, respectively. She received the Ph.D. degree in electrical and electronics engineering from the University of Melbourne, Australia, in 2015. From 2009 to 2011, she was with the Research and Development Team, Excel Technology, Sri Lanka. From 2015 to 2016, she was with the Department of Electrical and Computer Systems Engineering, Monash University, Australia. Currently, she is a Research Fellow with the Department of Electrical and Electronics Engineering, University of Melbourne, Australia. Her research interests are in cooperative communications and distributed antenna systems. She received the Melbourne International Research Scholarship and the Melbourne International Fee Remission Scholarship from the University of Melbourne.

Peter J. Smith (M'93–SM'01–F'15) received the B.Sc. degree in mathematics and the Ph.D. degree in statistics from the University of London, London, U.K., in 1983 and 1988, respectively. From 1983 to 1986, he was with the General Electric Company Hirst Research Centre, Telecommunications Laboratories. From 1988 to 2001, he was a Lecturer in statistics with the Victoria University of Wellington, Wellington, New Zealand. From 2001 to 2015, he was with the Department of Electrical and Computer Engineering, University of Canterbury, Christchurch, New Zealand. In 2015, he joined the Victoria University of Wellington as a Professor of Statistics. His research interests include the statistical aspects of design, modeling, and analysis for communication systems, cognitive radio, massive multiple-input multiple-output, and millimeter-wave systems.

Philippa A. Martin (S'95–M'01–SM'06) received the B.E. (Hons.) and Ph.D. degrees in electrical and electronic engineering from the University of Canterbury, Christchurch, New Zealand, in 1997 and 2001, respectively. She was a Post-Doctoral Fellow with the Department of Electrical and Computer Engineering, University of Canterbury, from 2001 to 2004. In 2002, she was a Visiting Research Fellow with the Department of Electrical Engineering, University of Hawaii at Manoa, Honolulu, HI, USA. Since 2004, she has been an Academic with the University of Canterbury, where she is currently a Professor. She served as an Editor of the IEEE TRANSACTIONS ON WIRELESS COMMUNICATIONS from 2005–2008, and she has been an Editor of the IEEE TRANSACTIONS ON WIRELESS COMMUNICATIONS since 2014. She regularly serves on technical program committees for IEEE conferences. Her current research interests include error correction coding, decoding and detection algorithms, equalization, space-time coding, cognitive radio, massive MIMO, UWB, smart grid, reconfigurable antennas, and cooperative communications in particular for wireless communications.

Jamie S. Evans (S'93–M'98) was born in Newcastle, Australia, in 1970. He received the B.S. degree in physics and the B.E. degree in computer engineering from the University of Newcastle, in 1992 and 1993, respectively, and the M.S. and the Ph.D. degrees in electrical engineering from the University of Melbourne, Australia, in 1996 and 1998, respectively. From 1998 to 1999, he was a Visiting Researcher with the Department of Electrical Engineering and Computer Science, University of California, Berkeley. Since returning to Australia in 1999, he has held academic positions with the University of Sydney, University of Melbourne, and Monash University. He is currently a Professor and the Deputy Dean with the Melbourne School of Engineering, University of Melbourne. His research interests are in communications theory, information theory, and statistical signal processing with a focus on wireless communications networks. He received the University Medal from the University of Newcastle and the Chancellor's Prize for excellence for his Ph.D. thesis.